

AD-A173 932

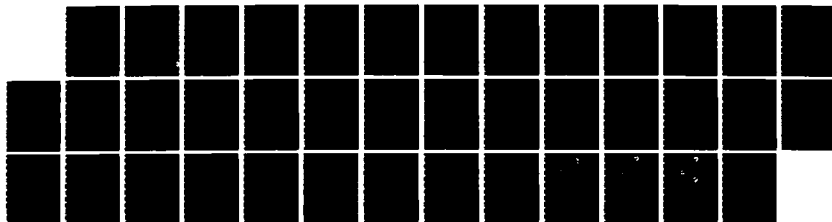
A MIXED-BASIS BAND STRUCTURE INTERPOLATION SCHEME
APPLIED TO THE ROCKSALT (U) CALIFORNIA UNIV LOS
ANGELES S KIM ET AL 15 OCT 86 TR-15 N00014-83-K-0612

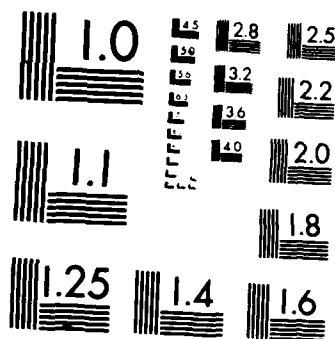
1/1

UNCLASSIFIED

F/G 28/12

NL





MICROCOPY RESOLUTION TEST CHART
NATIONAL BUREAU OF STANDARDS-1963-A

UNK
SECURITY

AD-A173 932

12

DOCUMENTATION PAGE

1a. REPORT SECURITY CLASSIFICATION UNCLASSIFIED		1b. RESTRICTIVE MARKINGS N/A													
2a. SECURITY CLASSIFICATION AUTHORITY N/A		3. DISTRIBUTION/AVAILABILITY OF REPORT Approved for public release; distribution unlimited													
2b. DECLASSIFICATION/DOWNGRADING SCHEDULE N/A															
4. PERFORMING ORGANIZATION REPORT NUMBER(S) N/A		5. MONITORING ORGANIZATION REPORT NUMBER(S)													
6a. NAME OF PERFORMING ORGANIZATION The Regents of the University of California	6b. OFFICE SYMBOL (If applicable)	7a. NAME OF MONITORING ORGANIZATION 1) ONR Pasadena - Administrative 2) ONR Alexandria - Technical													
6c. ADDRESS (City, State, and ZIP Code) Office of Contracts & Grants Administration U C L A, 405 Hilgard Avenue Los Angeles, CA 90024		7b. ADDRESS (City, State, and ZIP Code) 1) 1030 E. Green Street, Pasadena, CA 91106 2) 800 N. Quincy St., Arlington, VA 22217-5000													
8a. NAME OF FUNDING/SPONSORING ORGANIZATION Office of Naval Research	8b. OFFICE SYMBOL (If applicable) ONR	9. PROCUREMENT INSTRUMENT IDENTIFICATION NUMBER N00014-83-K-0612													
8c. ADDRESS (City, State, and ZIP Code) 800 N. Quincy Street, 614A:DHP Arlington, VA 22217-5000		10. SOURCE OF FUNDING NUMBERS <table border="1"><tr><td>PROGRAM ELEMENT NO.</td><td>PROJECT NO.</td><td>TASK NO.</td><td>WORK UNIT ACCESSION NO.</td></tr><tr><td></td><td></td><td></td><td></td></tr></table>		PROGRAM ELEMENT NO.	PROJECT NO.	TASK NO.	WORK UNIT ACCESSION NO.								
PROGRAM ELEMENT NO.	PROJECT NO.	TASK NO.	WORK UNIT ACCESSION NO.												
11. TITLE (Include Security Classification) UNCLASSIFIED: Tech.Rept.#15 - A MIXED-BASIS BAND STRUCTURE INTERPOLATION SCHEME APPLIED TO THE ROCKSALT STRUCTURE COMPOUNDS TiC, TiN AND TiO															
12. PERSONAL AUTHOR(S) Sehun Kim and R. Stanley Williams															
13a. TYPE OF REPORT Technical	13b. TIME COVERED FROM Feb '86 TO Oct '86	14. DATE OF REPORT (Year, Month, Day) 15 October 1986	15. PAGE COUNT 36												
16. SUPPLEMENTARY NOTATION															
17. COSATI CODES <table border="1"><tr><th>FIELD</th><th>GROUP</th><th>SUB-GROUP</th></tr><tr><td></td><td></td><td></td></tr><tr><td></td><td></td><td></td></tr><tr><td></td><td></td><td></td></tr></table>		FIELD	GROUP	SUB-GROUP										18. SUBJECT TERMS (Continue on reverse if necessary and identify by block number) Rocksalt compounds - band structure - first-principles calculations - ARPES and XRPS measurements - valence charge densities -- bonding effects	
FIELD	GROUP	SUB-GROUP													
19. ABSTRACT (Continue on reverse if necessary and identify by block number) <p>A mixed-basis band structure interpolation scheme has been applied to the rocksalt compounds TiC, TiN and TiO by fitting to first-principles calculations. For TiC and TiN, semi-empirical band structures were obtained by adjusting the interpolation parameters to improve the agreement between the calculated bands and data from previous Angle-Resolved Photoelectron Spectroscopy and K-ray Photoelectron Spectroscopy measurements. The use of the eigenfunctions to plot approximate valence charge densities to illustrate bonding effects is described.</p>															
20. DISTRIBUTION/AVAILABILITY OF ABSTRACT <input checked="" type="checkbox"/> UNCLASSIFIED/UNLIMITED <input type="checkbox"/> SAME AS RPT <input type="checkbox"/> DTIC USERS		21. ABSTRACT SECURITY CLASSIFICATION UNCLASSIFIED													
22a. NAME OF RESPONSIBLE INDIVIDUAL R. Stanley Williams		22b. TELEPHONE (Include Area Code) (213) 825-8818	22c. OFFICE SYMBOL UCLA												

DTIC FILE COPY

DTIC
SELECTE
NOV 12 1986

OFFICE OF NAVAL RESEARCH
Research Contract N00014-83-K-0612

TECHNICAL REPORT No. 15

A MIXED-BASIS BAND STRUCTURE INTERPOLATION SCHEME
APPLIED TO THE ROCKSALT STRUCTURE COMPOUNDS TiC, TiN and TiO

by

Sehun Kim and R. Stanley Williams

Department of Chemistry and Biochemistry
and Solid State Sciences Center
University of California, Los Angeles, CA 90024

Submitted for Publication

in

Physical Review B

(1986)

Accession For	
NTIS GRA&I	<input checked="" type="checkbox"/>
DTIC TAB	<input type="checkbox"/>
Unannounced	<input type="checkbox"/>
Justification	
By _____	
Distribution/ _____	
Availability Codes	
Dist	Avail and/or Special
A-1	

October, 1986

Reproduction in whole or part is permitted for
any purpose of the United States Government.



This document has been approved for public release and sale,
its distribution is unlimited

86 11 12 118

**A mixed-basis band structure interpolation scheme
applied to the rocksalt structure compounds TiC, TiN and TiO**

Sehun Kim and R. Stanley Williams

**Department of Chemistry and Biochemistry, and
Solid State Sciences Center
University of California, Los Angeles, CA 90024**

A mixed-basis band structure interpolation scheme has been applied to the rocksalt compounds TiC, TiN and TiO by fitting to first-principles calculations. For TiC and TiN, semi-empirical band structures were obtained by adjusting the interpolation parameters to improve the agreement between the calculated bands and data from previous Angle-Resolved Photoelectron Spectroscopy and X-ray Photoelectron Spectroscopy measurements. The use of the eigenfunctions to plot approximate valence charge densities to illustrate bonding effects is described.

I. Introduction

Mixed-basis band structure interpolation schemes (MBBSIS), which employ a combination of d-like orbitals and plane waves, have proven to be extremely valuable computational tools for examining the electronic structures of the d-band metals. Smith and various coworkers¹⁻⁴ have developed a fcc d-band interpolation scheme over the past decade and applied it as an aid in interpreting photoemission and UV reflectance data. An extension of Smith's scheme was utilized by Kim, et al.,⁵ to examine the band structure of several fluorite-structure compounds with d-states in the valence band. In this paper, the MBBSIS is applied to compounds with the rocksalt structure, and the use of the eigenfunctions to plot qualitative valence charge densities is illustrated.

The rocksalt structure can be described as a fcc Bravais lattice with a basis consisting of an A atom at (0,0,0) and a B atom at the position $(a/2)(1,0,0)$ of the conventional cubic cell. A large number of carbides, nitrides and oxides of the transition metals crystallize in the rocksalt structure. All carbides and nitrides of the Group IV and V transition metals have common properties: high melting point, hardness, brittleness and metallic conductivity. All of these physical properties are related to the electronic structure of the refractory compounds. The importance of the electronic structure for these compounds has motivated many theoretical and experimental investigations. General overviews of studies on the fourth and fifth

group transition metal carbides, nitrides and oxides are given in review articles^{6,7}

This investigation was motivated in part by the observation that the empirical pseudopotential method (EPM) calculations of the TiC electronic structure by Alward, et al.,⁸ who employed a nonlocal pseudopotential to treat the Ti d-states, produced valence charge densities that disagreed severely with those obtained from first-principles calculations⁹⁻¹¹ and experimental investigations.¹² The EPM calculations predicted that the local p-d charge density maximum near the carbon atom (the C 2s orbitals were not included in the calculation) was twice as large as that near the titanium atom, while the first principles calculations showed relatively comparable total (ie. including C 2s) charge densities around the two atoms. The intent of this study was to see if the MBBSIS could be used to obtain reliable band structures and also qualitatively correct charge densities for complex systems such as TiC, TiN and TiO. These systems have been studied extensively, and thus there exists a great deal of data to compare with the MBBSIS results.

Since the rocksalt structure has the same space group symmetry as fcc crystals, the same MBBSIS may be used for both lattices. The situation is similar to that for the previous study of the fluorite structure compounds.⁵ In that investigation, a MBBSIS similar to that of Smith, et al.¹⁻⁴ was used, except that more plane waves were included in the basis set.⁵ In Sec. II, the application of the MBBSIS

to the rocksalt structure compounds and the calculation of charge densities is described. In Sec. III, the energy bands, the total density-of-states (TDOS) and the electron density plots calculated by the MBBSIS are presented and discussed. Finally, Sec. IV contains the conclusions of this study.

II. Interpolation Scheme and Charge Density Calculations

Our method of calculation has been described previously.⁵ It is nearly identical to the MBBSIS of Smith,¹⁻⁴ except that the plane wave block of the Hamiltonian is a 39x39 submatrix, instead of a 16x16. The additional plane waves are required to represent the wavefunctions of the non-metal atom in the compound. The total local pseudopotential of the rocksalt compound AB can be written as follows:

$$V_{\underline{G}}(AB) = V_{\underline{G}}(A) + V_{\underline{G}}(B)\cos(\underline{G}\cdot\underline{\tau}), \quad (1)$$

where the d-bands originate from the A atom and $\underline{\tau} = (a/2)(1,0,0)$ is a vector connecting the transition metal atom (A) to the nonmetal atom (B) in the primitive unit cell. For the \underline{G} vectors of the reciprocal lattice of the rocksalt structure, the values of $\cos(\underline{G}\cdot\underline{\tau})$ are limited to ± 1 and determined only by the magnitude of \underline{G} , not its direction. Thus, the values of $V_{\underline{G}}$ for AB are all constants, with

$$V_{\underline{G}}(AB) = \begin{cases} V_{\underline{G}}(A) - V_{\underline{G}}(B) & \text{for } |\underline{G}| = \sqrt{3}, \sqrt{11} \\ V_{\underline{G}}(A) + V_{\underline{G}}(B) & \text{for } |\underline{G}| = 0, 2, \sqrt{8}, \sqrt{12}, \end{cases} \quad (2)$$

where $|\underline{G}|$ is in units of $2\pi/a$. As long as the d-orbital contribution of the B atoms to the band structure is negligible, the interpolation

Hamiltonian of the rocksalt structure is identical to that of the fcc structure.

The parameters of the MBBSIS for a particular system were determined by applying a nonlinear least squares method¹³ to fit the energy eigenvalues to those of first-principles calculations.¹⁴⁻¹⁶ The parameters usually converged to values that yielded average deviations (up to the tenth band of the rocksalt structure compounds) of about 0.2 eV after 5-6 iterations. Semi-empirical energy bands were then generated by adjusting the parameters of the MBBSIS to improve the agreement with available ARPES data for TiC^{14,17} and TiN.¹⁵ After the fitting parameters for a band structure were determined, a TDOS for the system was calculated by the method described previously.⁵

The electron density associated with each occupied state $E_{n,\underline{k}}$ can be defined as the square of its eigenfunction:

$$\begin{aligned} \rho_{n,\underline{k}}(\underline{x}) &= \psi_{n,\underline{k}}(\underline{x})^2 \\ &= \left(\sum_i b_i^n \phi_{i,\underline{k}}(\underline{x}) + \sum_j c_j^n d_{j,\underline{k}}(\underline{x}) \right)^2 \end{aligned} \quad (3)$$

where $\phi_{i,\underline{k}}(\underline{x})$ and $d_{j,\underline{k}}(\underline{x})$ are the 39 Orthogonalized Plane Waves (OPW) and the 5 d-wave functions, respectively, and b_i^n and c_j^n are the coefficients of the basis functions that result from diagonalizing the MBBSIS Hamiltonian at point \underline{k} in the BZ. The set of OPWs is given by

$$\phi_{i,\underline{k}}(\underline{x}) = a_i^{-1}(|\underline{k}_i\rangle - \sum_j |d_j\rangle \langle d_j | \underline{k}_i \rangle). \quad (4)$$

where the plane wave $|\underline{k}_i\rangle = \Omega^{-1/2} e^{i\mathbf{k} \cdot \mathbf{r}}$, Ω is the primitive unit cell volume, and $a_i = [1 - \sum_j |\langle d_j | \underline{k}_i \rangle|^2]^{1/2}$. In the present charge density calculations, since the contribution of the orthogonalization terms in eq. (4) was negligible, the $\phi_{i,\underline{k}}(\underline{x})$ were approximated as being simply plane waves normalized to a charge density of two electrons per primitive unit cell. The five d-wave functions ($d_{xy}, d_{yz}, d_{xz}, d_{x^2-y^2}$ and $d_{3z^2-x^2}$) can be written as

$$d_{j,\underline{k}}(\underline{x}) = R_{3d}(\underline{x}) Y_{2j}(\underline{k}), \quad (5)$$

where $R_{3d}(\underline{x})$ is the radial part of the d-wave functions and the $Y_{2j}(\underline{k})$ are properly normalized spherical harmonics. In the MBBSIS calculations employed, no explicit form for the radial part of the d-wave function was used. An alternative form of the interpolation scheme, which incorporated Slater radial d-wave functions and used the orbital exponent as a fitting parameter, as in Ref. 5, was tested. However, simply using Smith's form for the Hamiltonian terms of the MBBSIS, then substituting the single-zeta radial wave function for Ti 3d taken from Clementi and Roetti's tables¹⁸ into Eq. 3, produced charge densities nearly identical with those calculated using the alternative scheme.

The electron density calculated as a function of \underline{r} for an arbitrary \underline{k} -point does not necessarily have the symmetry of the crystal. Imposing the crystal symmetry on the charge density can be accomplished by either summing $\rho_{n,\underline{k}}(\underline{r})$ over the star of \underline{k} or applying the appropriate space group operations on $\rho_{n,\underline{k}}(\underline{r})$. In the calculations reported here, the 48 space group operations of O_h were applied to the charge density calculated at each value of \underline{k} . This procedure was computationally faster than evaluating $\rho_{n,\underline{k}}(\underline{r})$ over the star of \underline{k} , and yielded the same results. Total valence charge densities were calculated by summing over all the valence bands at 10 special \underline{k} -points¹⁹. A large number of simplifications and approximations have been used to calculate these charge densities. The primary value of such calculations, as long as they are qualitatively correct, is to be able to visualize the electronic structure of a relatively complex system in real space (ie. a bond picture of the system) without resorting to extremely expensive computations or requiring an enormous first-principles basis of eigenvectors.

All the calculations were performed using a VAX 11/780 computer. The Central Processing Unit (CPU) time of the VAX required to produce the eigenvalues at a single \underline{k} -point was 3.7 sec., and a value of the charge density at a particular \underline{r} for a band state $E_{n,\underline{k}}$ required 0.3 sec.

III. Results and Discussion

Since relativistic effects are small for the 3-d transition metals, the MBBSIS calculations for the Ti compounds were performed without including a spin-orbit parameter. Most of the energy band calculations for the transition metals of group IV and V reviewed in Refs. [6,7] were limited to no higher in energy than the tenth energy band. Recently, Linearized Augmented Plane Wave (LAPW) calculations^{14,15} for TiC and TiN generated band structures up to 35 eV above the Fermi energy (E_F). The MBBSIS was used to fit these LAPW energy bands up to the twelfth and part of the thirteenth bands (18 eV above E_F) using 45~50 LAPW energy eigenvalues at 4~5 high symmetry points in the BZ. Since the LAPW N 2s bands were omitted in Ref. 15, the N 2s bands of the MBBSIS were initially fitted to those of the APW calculations by Neckel et al.²⁰ The average deviation from the LAPW energy bands was ~0.5 eV for TiC and TiN. These values are ~3 times larger than the average deviation for fits to the TiO band structure, since the APW calculations for this compound did not include eigenvalues above the tenth band. The MBBSIS for TiO was fitted to the early band structure of Ern and Switendick¹⁶ because these authors listed their eigenvalues in a Table and thus made possible a more precise comparison with a previously calculated band structure. However, the band structure plot of Ref. 16 agreed very well with that shown by Neckel, et al. in a more recent publication.²⁰

The most severe deviations of the MBBSIS energy bands from the LAPW eigenvalues occurred at the second band of Γ_1 and the first band of Γ_2 symmetry, and the largest contributions to the average deviation come from energies above the tenth band for TiC and TiN. The agreement for the ten bands lowest in energy was generally within 0.2 eV. In the case of TiO, for which energy bands were generated only up to the tenth band in Fig. 3, the average deviation from the APW energy bands¹⁶ was comparable to the results of a fit to an improved LCAO method that used 45 disposable parameters.²¹ Thus, the MBBSIS is able to fit the rocksalt-compound bands as well as the LCAO method with fewer parameters.

The TDOS for Ti compounds calculated by the MBBSIS agreed very well those with calculated from LCAO bands fitted to APW results²⁰⁻²¹ (see Figs. 1-3). Most of the experimental studies to date have provided information about the TDOS of these compounds, but do not contain k-resolved information about the band structures. In recent studies, however, detailed band mapping was performed using ARPES to obtain information about band dispersions and surface states for TiC^{14,17} and TiN.¹⁵ These data allowed direct comparison between calculated band structures and ARPES results. Noticeable discrepancies between the LAPW calculations and ARPES data can be found. The second band of Δ_1 symmetry and the first band of Δ_5 symmetry calculated by the LAPW technique lie closer to the Fermi level than those determined from ARPES data for TiC and TiN. For example, in the case of TiN, the experimentally determined position

of the Γ_{15} point is $-3.4(\pm 0.1)$ eV, of the X_5 point $-4.0(\pm 0.2)$ eV, and of the X_4 point $-6.4(\pm 0.2)$ eV¹⁵, compared with calculated values of -2.2 , -3.3 , and -5.9 eV,²¹ respectively. Also, the LAPW energy bands for TiN¹⁵ along Γ -X did not show a gap between the first band of Δ_5 and the first band of Δ_2 , symmetry along the Δ direction, but the ARPES results indicated a substantial gap¹⁵ (see Fig. 4).

The MBBSIS bands of TiC and TiN, which were initially fitted to the LAPW energy bands,^{14,15} were adjusted to agree with the experimental results.^{15,17} The resulting band structures and TDOS plots are shown in Fig. 1 and 2 for TiC and TiN, respectively, and the MBBSIS results for TiO are shown in Fig. 3. The empirically adjusted energy bands for TiN agree very well with the ARPES data along Γ -X and show clear a band gap between the third (Δ_5) and fourth (Δ_2) bands, as shown in Fig. 4.

The possible caveat to adjusting the valence bands to agree with photoemission data is that such bands may not reflect the true ground-state electronic structure of the compounds. However, comparison of the band structures of Ag determined from photoemission and first-principles calculations shows an average deviation of approximately 0.2 eV in the absolute locations of the valence bands,²² and thus the photoemission results should represent ground-state bands to within the uncertainty of the MBBSIS procedure.

A common method of determining the quality of band structure

calculations is to compare the TDOS to spectral features in valence band XPS spectra.²³⁻²⁵ In order to make a direct comparison with XPS spectra, TDOS curves were produced with a 1.0 eV Gaussian broadening to account for lifetime and instrumental resolution effects. The overall agreement with the corresponding XPS spectra was good, as shown in Fig. 5. The detailed differences between the XPS spectra and the TDOS curves calculated from bands fitted to LAPW results may be caused by photoemission cross section effects or by inaccuracies in the LAPW bands. The TDOS calculated using the empirically adjusted bands for TiN shows a significantly improved agreement with the XPS spectrum²⁴ (see Fig. 5). For TiC, the agreement between the empirical TDOS and the XPS spectrum was also improved with respect to the bands fitted to the LAPW results, but there were still some pronounced differences. This may have been because fewer experimental ARPES data¹⁹ for TiC were available to use in fitting the MBBSIS.

A decomposition of the Ti d-like TDOS into t_{2g} and e_g manifolds provides interesting information about the nature of the occupied states. From the partial DOS calculated by the MBBSIS, the number of occupied Ti t_{2g} and e_g states is about equal for TiC, whereas there are more occupied t_{2g} than e_g states in both TiN and TiO. Also, the partial DOS analysis showed that the d-like contribution to the nonmetal 2p-band decreased in the series TiC, TiN and TiO. This indicates that the intermixing between nonmetal p and metal d orbitals, or the degree of covalency, decreased going from TiC to

TiO. This agrees with the qualitative pictures obtained from the electron densities. Blaha, et al.¹³ compared the electron densities of TiC and TiN calculated from LAPW wave functions with the X-ray diffraction experiments of Dunand, et al.¹⁴ In this comparison, the nonspherical charge density around the titanium atom determined from the calculation and the diffraction data agreed very well.

Studies of chemical bonding in the Ti rocksalt compounds based on first-principles calculations revealed a combination of ionic, covalent and metallic contributions. Electron density plots may be used to show pictures of the orbital overlap or p-d interactions, in order to visualize the chemical bonding of these compounds. The total valence electron densities of TiC, TiN and TiO calculated by the MBBSIS fitted to the first-principles bands¹⁴⁻¹⁶ agree qualitatively with the first-principles results of Ref. 9, even with all the approximations discussed in Sec. II. The MBBSIS electron density plots for TiC, TiN, and TiO exhibit all the same features as those shown in Fig. 3 of Ref. 9. The electron densities around the non-metal atoms are spherically symmetric and show increased localization going from TiC to TiO (Fig. 6). The electron densities around the titanium atom strongly deviate from spherical symmetry, and the deviation changes from e_g symmetry for TiC to t_{2g} symmetry for TiO.

The e_g symmetry for the Ti electron density in TiC agrees with that of Blaha, et al.,⁹ but differs from that of Trebin and Bross.¹⁰

The latter charge density was calculated using the Modified Augmented Plane Wave (MAPW) method, and indicated a t_{2g} symmetry of the electron charge density at Ti. This discrepancy was discussed by Blaha, et al., who used 29 k-points chosen over a uniform grid in the irreducible 1/48 of the BZ to calculate the charge density in Ref. 26. The present study confirms that the difference in the symmetry of the charge density is caused by the identity of the eigenfunctions used in k-summation for calculating the total valence electron densities. When the total valence electron densities were calculated with the MBBSIS wave functions using the same k-points as Trebin and Bross,¹⁰ the resulting plot showed t_{2g} symmetry at the Ti atom. However, the total valence electron densities calculated using 2, 10 and 60 special k-points¹⁹ all had e_g symmetry about the Ti atom, and they were nearly identical to one another. Thus, choosing the correct k-points for calculating properties such as valence electron densities is extremely important, but when using the special points of Chadi and Cohen,¹⁹ only a small number of k-points are required. The fact that the MBBSIS wave functions successfully reproduced the chemical trends seen for the symmetry of the electronic charge about the Ti atom for these compounds indicates that they can be useful in qualitative examinations of charge densities, especially if first principles wave-functions are not available.

When the total charge densities of the MBBSIS fitted to LAPW results were quantitatively compared with the first principles

results, significant differences were apparent. The differences were particularly acute at the mid-point of the Ti-nonmetal bond. In the case of TiC, the values of the total charge densities mid-way between Ti and C are 8 and 20.7 e/Å from the first principles results and the MBBSIS, respectively, but the maximum charge densities close to each atom differ by less than ~10 %. Thus, the MBBSIS charge densities display less localization than the first principles results, which is likely the result of using such a small number of plane waves in the basis. However, the relative magnitudes of the MBBSIS total charge density maxima near Ti and the non-metal atom for the three compounds agreed very well with the first principles results.⁹

It is also interesting to compare the electron density plots of the empirically adjusted bands with those of the LAPW fitted bands for TiC and TiN.²⁷ By comparing the MBBSIS charge densities with each other, the consequence of correcting the first principles band structure to agree with experiment should be evident. In TiC, the empirically adjusted MBBSIS charge density is higher at the Ti atom and lower at the C atom than the MBBSIS density directly fitted to the LAPW bands. This suggests that the experimental results indicate more covalent bonding character in TiC than predicted by the LAPW calculations. In TiN, contrary to the TiC result, the adjusted MBBSIS shows a lower electron density at the Ti atom and higher electron density at the N atom. Therefore, TiN is somewhat more ionic than the LAPW calculation¹¹ indicates. This is compatible with the fact that the N-2p energy band determined from ARPES data¹⁷

resides about 1 eV further below the Fermi energy than that of the LAPW energy band and the experimentally determined band dispersions are smaller than the calculated ones.

An X-ray diffraction experiment yields the total electron density, but an energy band calculation can provide a partitioning of electron density into contributions from individual bands. The electron density plots of each band for selected k-points can be used to visualize various types of bonding character, which leads to an improved understanding of the bonding properties of the compounds.

By comparing MBBSIS charge densities of different compounds, qualitatively correct chemical trends should be evident. The relationship between banding and bonding may be illustrated by examining states with k-points along the Δ direction. There are two pairs of bands with the same symmetry Δ_1 (from nonmetal 2p and Ti e_g bands) and Δ_5 (from nonmetal 2p and Ti t_{2g} bands), as well as a single Δ_2 band (from Ti t_{2g}) and a Δ_2 band (from Ti e_g). The interaction between the states of the same symmetry mixes the Δ_1 states to form $p-e_g$ hybrids (pd_σ bonding) and the Δ_5 states to form $p-t_{2g}$ hybrids (pd_π bonding). In Fig. 7, the electron density plots for the first band with Δ_5 symmetry for the three Ti compounds illustrate the covalent bonding (pd_π) between nonmetal 2p and Ti t_{2g} orbitals. The electron densities around the Ti atoms are reduced going from TiC to TiO, while those around the nonmetal atoms increase. This indicates that TiC exhibits the highest degree of

covalent bonding and that ionic character increases as the series progresses from TiC to TiO.

The electron density plots at the Fermi energy are illustrated in Fig. 8. Three bands cross the Fermi level in TiC and one band in TiN and TiO along the Δ line. In TiC, the electron density plot of the first Δ_5 band at the Fermi energy reveals a slight σ -type covalent bonding character between the C and Ti atoms. In TiN and TiO, the electron density plots of the second band with Δ_5 symmetry at the Fermi level show predominantly metal-metal interactions (Ti dd_σ and 4s in character). These plots are important since they involve the electronic states that contribute most to the conductivity of these compounds. Thus, these charge densities indicate that for the perfect materials (i.e. those for which defects do not dominate the charge transport properties) the Ti atoms would be primarily responsible for electron transport in the Ti rocksalt compounds, with the nonmetals acting essentially as spectators that hold the crystal together by ionic forces. By examining the charge density at the Fermi level, the importance of Ti-Ti interactions becomes much more evident, since the total valence charge density is dominated by states localized near the Ti and nonmetal atoms.

The disposable parameters determined from the fitting procedure for the rocksalt compounds are listed in Table I, along with the standard deviation for each parameter. The A parameters, which are

essentially three center integrals involving the Ti 3d orbitals, seem to vary without trends from TiC to TiO. Most of the A parameters are essentially zero; their absolute values are less than their standard deviations. This is expected, since the Ti atoms are separated by fairly large distances in the rocksalt compounds, and thus the direct d-d interactions should be relatively small. The much larger values of the E_0 and Δ parameters in comparison with those of the fcc metals might be the result of compensating for the large hybridization parameters B_t and B_e , which are affected by the t_{2g} and e_g band positions.

Unfortunately, the parameters in the MBBSIS do not appear to have a strong physical basis. Depending on the starting guesses in the fitting procedure, band structures that are nearly identical can arise from parameter sets with extremely different values. The wave functions that result from such different parameters are also very similar, and produce essentially identical charge densities. Thus, it appears as though the MBBSIS for rock-salt type compounds is over determined using Smith's parameterization,¹⁻⁴ and that schemes with different parameters are worth exploring; in particular schemes that involve only 3 parameters for the direct d-d interactions¹ and additional pseudopotential and orthogonalization terms as well as an increased number of plane waves should substantially improve the MBBSIS fit and make the parameters more physically meaningful.

IV. Conclusion

The MBBSIS for fcc d-band metals was extended to include the rocksalt structure compounds. The band structures for TiC, TiN and TiO fitted by the present scheme were in good agreement with the first-principles calculations up to the tenth band, with an average deviation of ~ 0.2 eV. Semi-empirical band structures for TiC and TiN were also obtained by adjusting the interpolated energy bands to agree with ARPES data. This procedure assumes that the photoemission data provide a good picture of the ground-state band structure. The TDOS curves generated using the empirically adjusted bands of TiC and TiN demonstrated better agreement with XPS valence band spectra than the MBBSIS bands fitted to the first-principles results. Even though the approximations used for the Ti d-orbital contribution to the MBBSIS wave functions were extreme, the valence electron density plots calculated by using the MBBSIS bands agreed qualitatively very well with the first principles results of Blaha and Schwartz.⁹ The MBBSIS charge densities showed much better agreement with those first principles results than did either the EPM results of Ref. 8 or the first principles calculation of Ref. 10.

The MBBSIS charge densities were used to illustrate several points. The valence electron density plots of the individual bands showed an increasingly ionic bonding contribution in the series TiC, TiN and TiO. The metal-metal bonding is similar in all these compounds, and is most pronounced for energy bands at the Fermi

level. Comparison of charge densities calculated from the MBBSIS fitted to first principles results and the empirically adjusted bands showed that TiC involves more covalent bonding than predicted by the first principles calculations, whereas TiN is more ionic.

V. Acknowledgments

This work was supported by the Office of Naval Research. One of us (RSW) acknowledges the Camille and Henry Dreyfus Foundation and the Alfred P. Sloan Foundation for financial support. We are grateful to D. J. Chadi for enlightening discussions.

VII. References

1. N.V. Smith and L.F. Mattheiss, Phys. Rev. B 9, 1341 (1974).
2. N.V. Smith, Phys. Rev. B 19, 5019 (1979).
3. R. Lasser, N.V. Smith, and R.L. Benbow, Phys. Rev. B24, 1875 (1981).
4. R.L. Benbow and N.V. Smith, Phys. Rev. B 27, 3144 (1983).
5. S. Kim, J.G. Nelson and R.S. Williams, Phys. Rev. B 31, 3460 (1985).
6. J.L. Calais, Adv. Phys. 26, 847 (1977).
7. A. Neckel, Int. J. Quantum. Chem. 23, 1317 (1983).
8. J.F. Alward, C.Y. Fong, M. El-Batanouny and F. Wooten, Solid State Comm. 17, 1063 (1975).
9. P. Blaha and K. Schwartz, Int. J. Quantum Chem. 23, 1535 (1983).
10. H.R. Trebin and H. Bross, J. Phys. F: Met. Phys. 14, 1453 (1984).
11. P. Blaha, J. Redinger and K. Schwartz, Phys. Rev. B 31, 2316 (1985).
12. A. Dunand, H.D. Flack and K. Yvon, Phys. Rev. B 31, 2299 (1985).
13. L.F. Mattheis, Phys. Rev. B 5, 290 (1972).

14. A. Callenas, L.I. Johansson, A.N. Christenson, K. Schwartz and J. Redinger, Phys. Rev. B 27, 5934 (1983).
15. L.I. Johansson, A. Callenas, P.M. Stefan, A.N. Christenson and K. Schwartz, Phys. Rev. B 24, 1883 (1981)
16. V. Ern and A.C. Switendick, Phys. Rev. 137, A1927 (1965)
17. J.H. Weaver, A.M. Bradshaw, J.F. van der Veen, F.J. Himpsel, D.E. Eastman and C. Politis, Phys. Rev. B 22, 4921 (1980).
18. E. Clementi and C. Roetti, At. Data Nucl. Data. Tables 14, 177 (1974).
19. D.J. Chadi and M.L. Cohen, Phys. Rev. B 8, 5747 (1973).
20. A. Neckel, P. Rastl, R. Eibler, P. Weinberger and K. Schwartz, J. Phys. C : Solid State Phys. 12, 5453 (1979).
21. M. Dorrer, R. Eibler and A. Neckel, Theoret. Chim. Acta (Berl.) 60, 313 (1981).
22. J.G. Nelson, S. Kim, W.J. Gignac, R.S. Williams, J.G. Tobin, S.W. Robey, and D.A. Shirley, Phys. Rev. B 32, 3465 (1985).
23. A.L. Hagstrom, L.I. Johansson, B.E. Jacobsson and S.B.M. Hagstrom, Solid State Comm. 19, 647 (1976).
24. H. Hochst, R.D. Bringans, P. Steiner and Th. Wolf, Phys. Rev. B 25, 7183 (1982).

25. G.K. Wertheim and D.N. Buchanan, Phys. Rev. B 17,
2780 (1978).
26. P. Blaha, K. Schwartz and J. Redinger, J. Phys. F: Met. Phys.
15, 263 (1985).
27. S. Kim and R.S. Williams, J. Vac. Sci. Technol. A 4, 1603 (1986).

Table I. Parameters used in the MBBSIS.^a

Parameters	TiC		TiN		TiO	
	LAPW fitted ^b	empirical ^c	LAPW fitted ^b	empirical ^c	LAPW fitted ^b	APW fitted ^b
E ₀	19.46 ± 0.4	19.32 ± 0.4	18.12 ± 0.4	19.43 ± 0.3	24.53 ± 0.6	
Δ	-4.231 ± 0.7	-1.901 ± 0.6	-4.253 ± 0.6	-5.426 ± 0.5	-7.822 ± 0.9	
A ₁	0.0725 ± 0.2	0.1025 ± 0.2	0.1566 ± 0.2	0.0752 ± 0.2	-1.065 ± 0.2	
A ₂	-0.0451 ± 0.2	-0.0154 ± 0.2	-0.0214 ± 0.1	-0.1366 ± 0.1	-0.3124 ± 0.2	
A ₃	0.2697 ± 0.2	0.1533 ± 0.2	0.2238 ± 0.2	-0.2510 ± 0.5	-0.2510 ± 0.5	
A ₄	-0.0488 ± 0.2	0.0495 ± 0.1	-0.0114 ± 0.1	-0.0332 ± 0.1	-0.2308 ± 0.2	
A ₅	0.0328 ± 0.1	0.0159 ± 0.1	0.0458 ± 0.1	0.0487 ± 0.1	0.0818 ± 0.1	
A ₆	-0.1484 ± 0.2	-0.0547 ± 0.1	-0.0310 ± 0.2	-0.5759 ± 0.3	-0.5759 ± 0.3	
S	12.19 ± 4	-0.52 ± 3	-4.89 ± 4	-0.18 ± 3	1.41 ± 3	
B _t	47.39 ± 2	48.54 ± 1	44.75 ± 2	50.62 ± 2	50.62 ± 2	
B _e	22.90 ± 2	36.96 ± 2	21.81 ± 2	***	21.81 ± 2	
α	0.0974 ± 0.001	0.0983 ± 0.002	0.0916 ± 0.001	0.0901 ± 0.001	0.0793 ± 0.001	
R	0.2043 ± 0.005	0.1900 ± 0.005	0.1978 ± 0.007	0.2342 ± 0.005	0.2341 ± 0.005	
V ₀₀₀	5.295 ± 0.3	3.047 ± 0.3	6.625 ± 0.3	6.037 ± 0.2	-1.918 ± 0.2	
V ₁₁₁	4.333 ± 0.1	3.754 ± 0.1	7.594 ± 0.1	7.412 ± 0.1	3.647 ± 0.1	
V ₂₀₀	-1.288 ± 0.2	-1.109 ± 0.2	1.753 ± 0.2	1.364 ± 0.1	-2.135 ± 0.2	
V ₂₂₀	-1.331 ± 0.2	-1.284 ± 0.3	0.8423 ± 0.2	***	-1.140 ± 0.2	
V ₃₁₁	-2.123 ± 0.2	-3.045 ± 0.2	-0.4085 ± 0.2	***	-0.5987 ± 0.2	
V ₂₂₂	3.394 ± 0.3	0.2510 ± 0.7	4.002 ± 0.4	***	2.471 ± 0.3	
E _f ^d	8.653	***	9.251	***	8.802	
lattice constant	4.330		4.241		4.181	
average deviation ^e	0.461	0.171	0.306	0.224	0.198	

^aAll values in eV except R in a reduced unit ($4a/\pi$) and the lattice constant in Å. The ± sign indicate the standard deviation of each parameter. The parameters are intentionally reported with more significant figures than justified by the standard deviations in order to produce band structures that are essentially identical with those shown in Fig. 1-3.

^bParameters are fitted to LAPW or APW eigenvalues from Ref. 14, 15 and 16 for TiC, TiN and TiO, respectively.

^cParameters are empirically adjusted to fit ARPES data from Ref. 17 and 15 for TiC and TiN, respectively.

^dTaken from Ref. 16, these offset are used to define the Fermi energy as the zero of the energy scale for each band structure.

^eFor deviations up to the tenth band except those of LAPW fitted parameters for TiC and TiN up to the thirteenth band.

FIGURE CAPTIONS

Fig. 1. Semi-empirical energy bands that have been adjusted to improve agreement with the ARPES data of Ref. 17 and the corresponding TDOS curve. The energy scale is referenced to the Fermi energy and the TDOS scale is in electrons of one spin per eV per unit cell volume.

Fig. 2. Semi-empirical energy bands that have been adjusted to improve agreement with the ARPES data of Ref. 15 and the corresponding TDOS curve with the same remarks as Fig. 1.

Fig. 3. Interpolated energy bands that have been fitted to the first-principles calculation of Ref. 16 and the corresponding TDOS curve with the same remarks as Fig. 1.

Fig. 4. The comparison of the semi-empirical and first-principles energy bands with the ARPES data of Ref. 15 along the Δ line of the BZ for TiN. The solid lines are the semi-empirical energy bands calculated by the MBBSIS, and the dashed lines are the first-principles energy bands. The circles and boxes represent the ARPES data of Ref. 15, with the former corresponding to direct transitions and the latter to perhaps indirect transitions or surface features.

Fig. 5. Comparison between the TDOS curves of TiC, TiN and TiO and

the corresponding XPS spectra in Ref. 23-25 with a piecewise linear background subtracted. The dots represent the adjusted XPS data. The TDOS curves of the semi-empirical band structures are shown as solid lines. The TDOS curves of the interpolated band structures fitted to the first-principles calculations are represented as dashed lines. All curves are plotted versus binding energy referenced to the Fermi energy.

Fig. 6. Total valence electron density plots for (a) TiC, (b) TiN and (c) TiO in the (100) plane corresponding to the band structures of Fig. 1-3, calculated by summing over valence bands for 10 special k-points and normalized to 8, 9 and 10 electrons per primitive unit cell, respectively. The contour lines represent intervals of electron density of 1 e/Ω.

Fig. 7. Electron density plots of (a) TiC, (b) TiN and (c) TiO of the first band with Δ_5 symmetry at $k = (2\pi/a)(0.5, 0, 0)$ in the (100) plane. Each density is normalized to 2 e/Ω, and the contour lines represent intervals of electron density of 0.5 e/Ω.

Fig. 8. Electron density plots of (a) TiC, (b) TiN and (c) TiO for the band with Δ_5 symmetry at the k-point at which the band crosses the Fermi energy in Fig. 1-3, respectively. Each density is normalized to 2 e/Ω, and the contour lines represent intervals of electron density of 1 e/Ω.

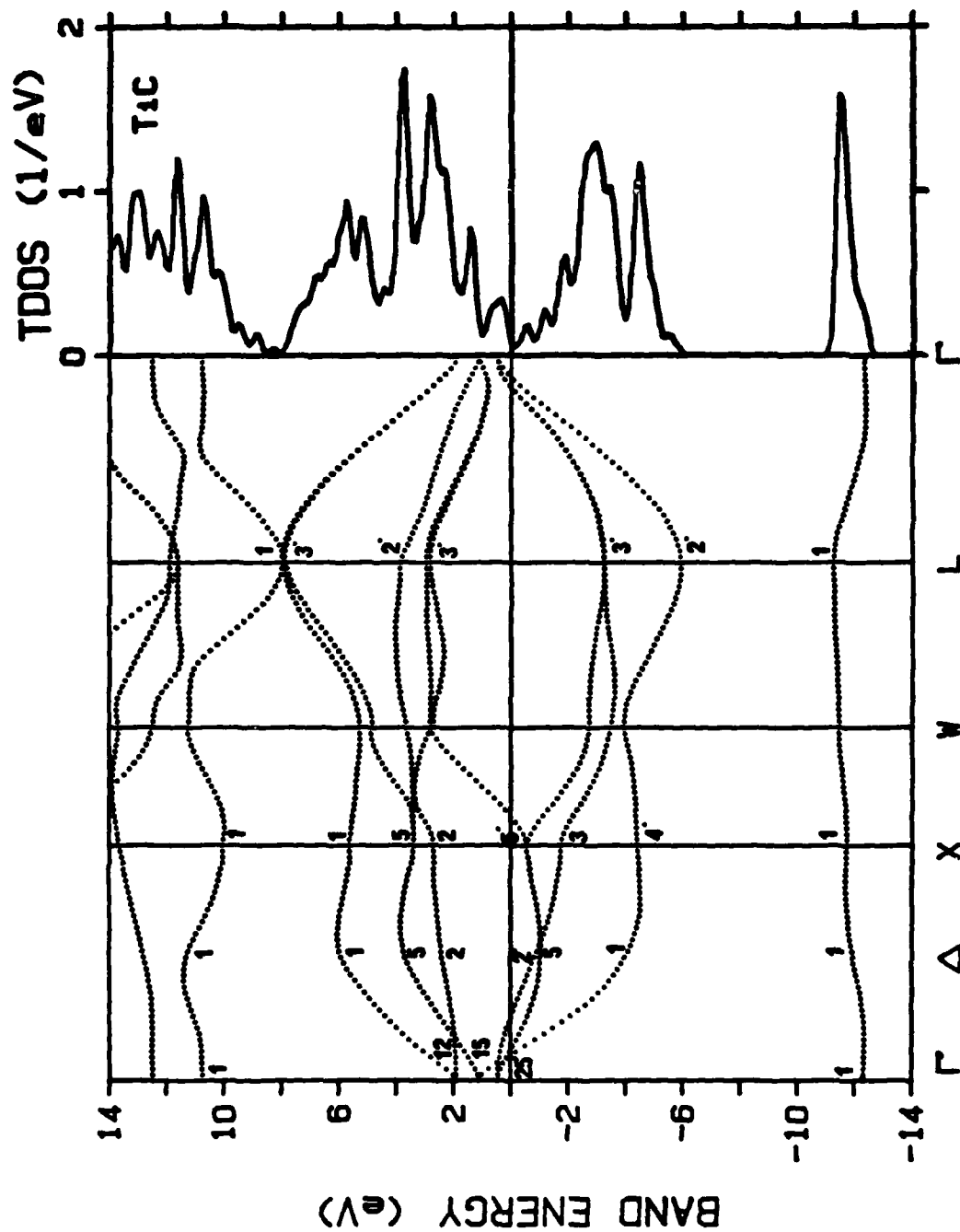


FIG. 1

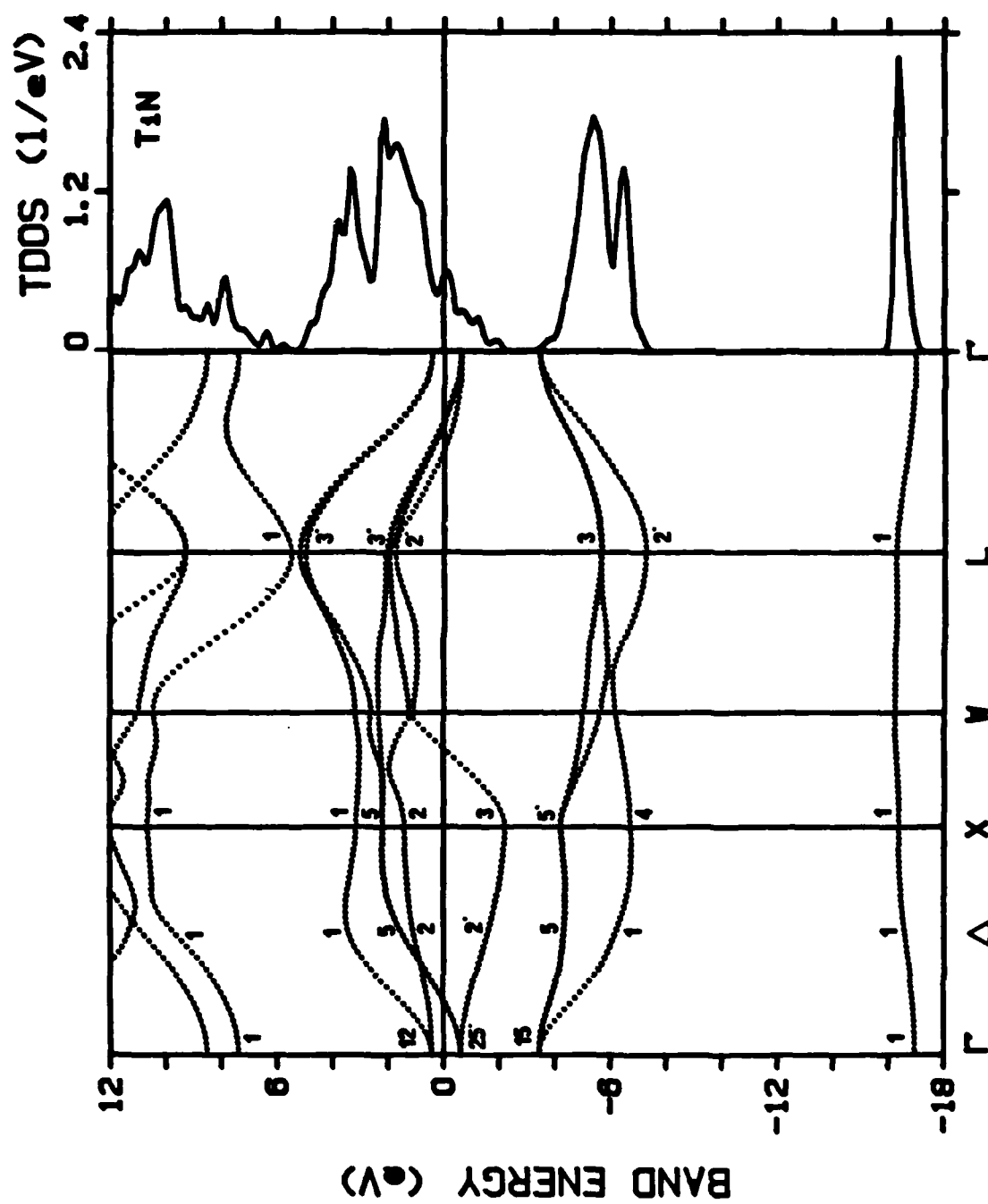


FIG. 2

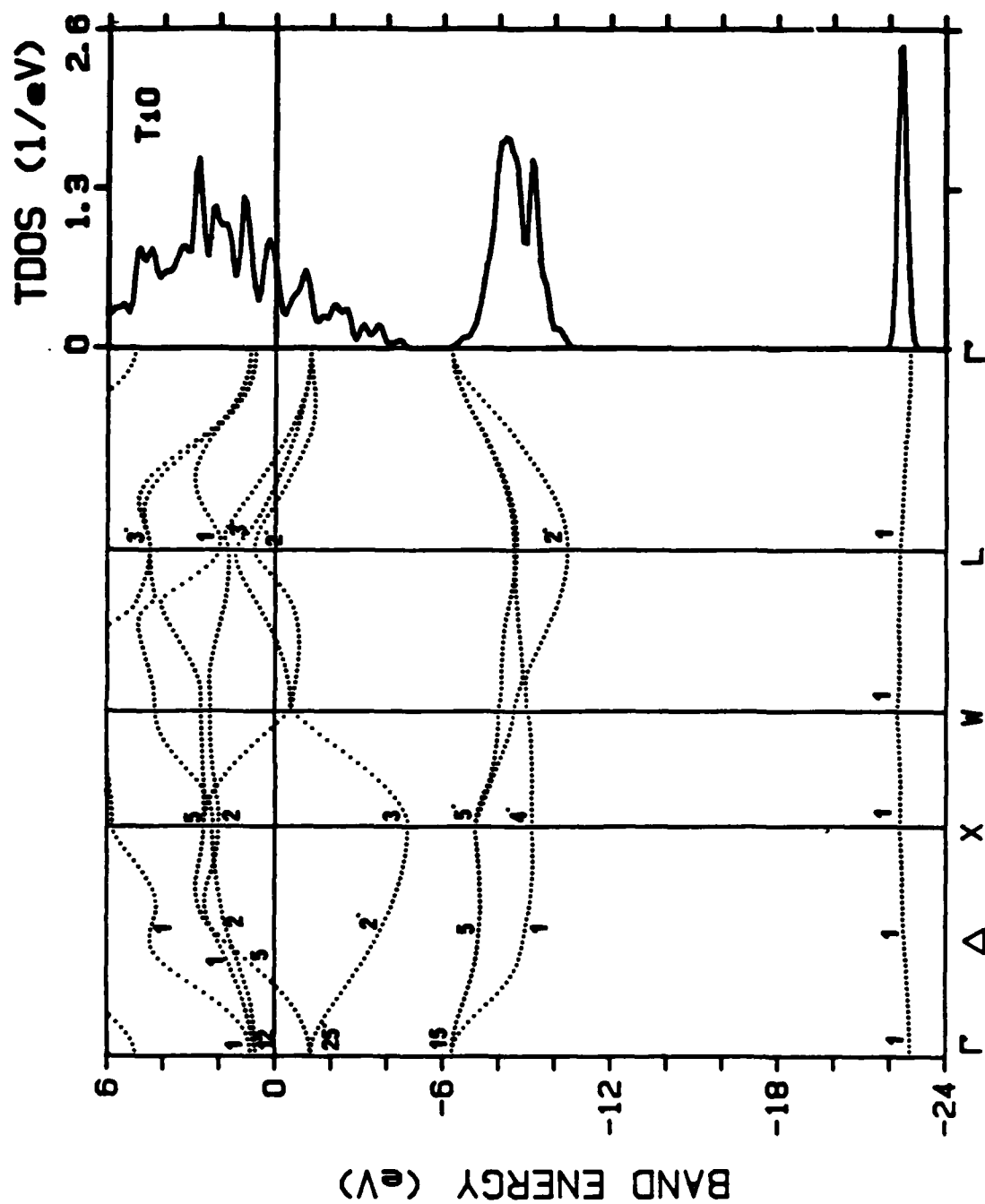


FIG. 3

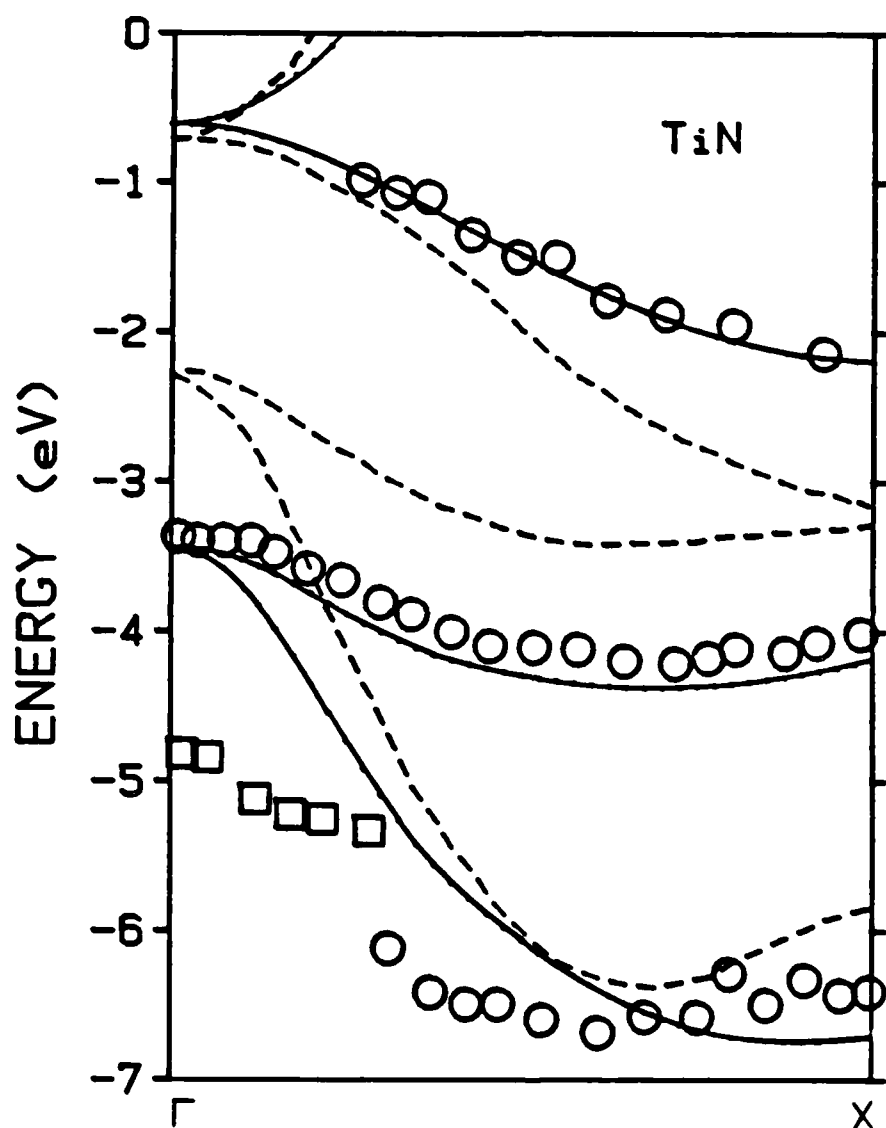


FIG. 4

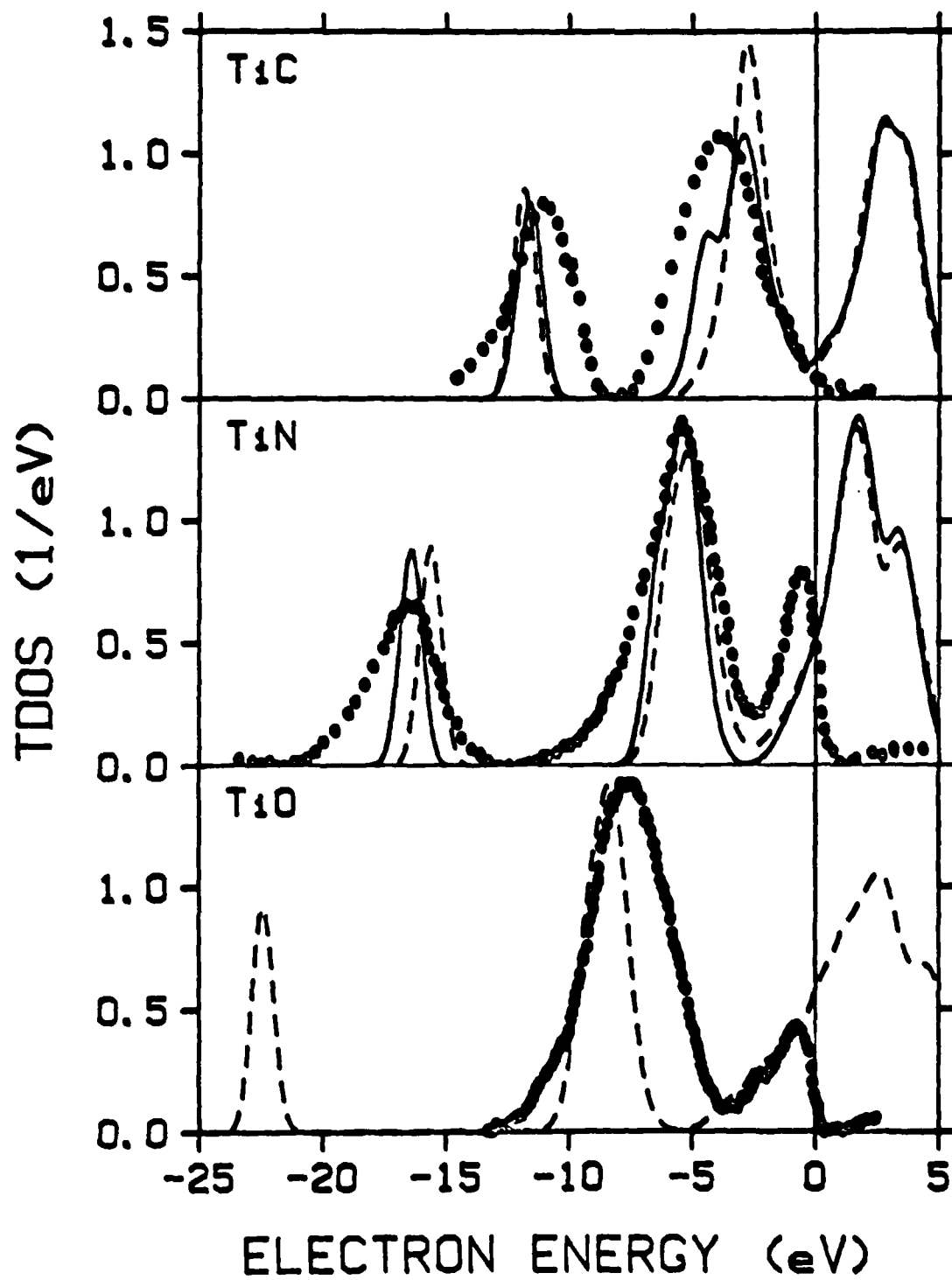


FIG. 5

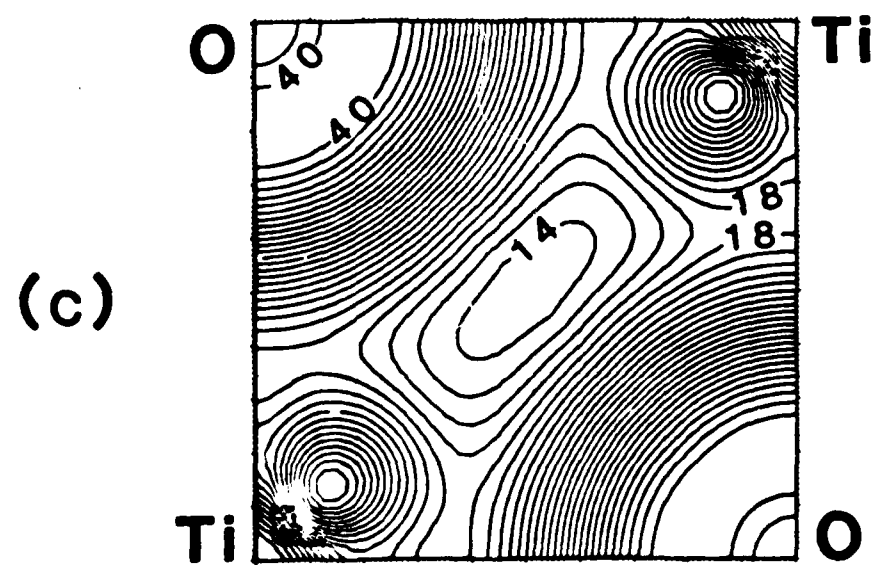
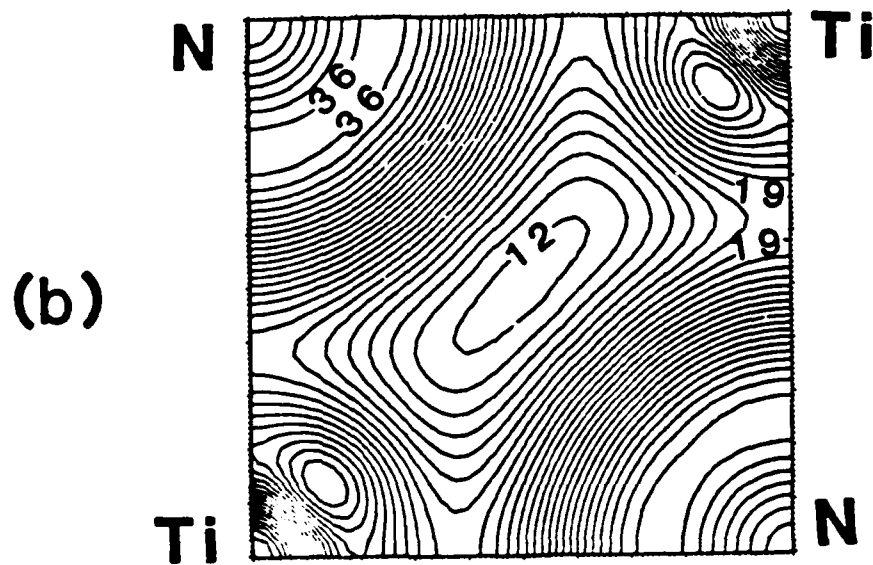
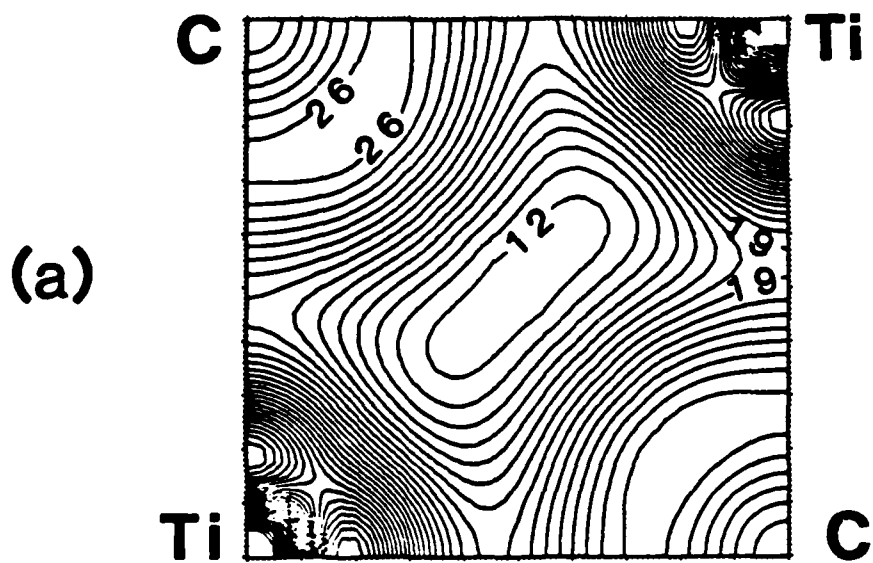


FIG. 6 34

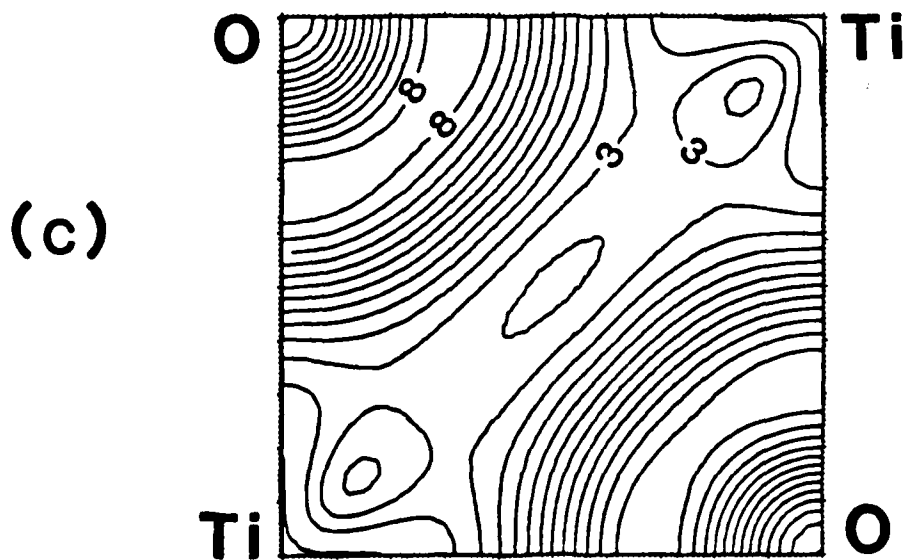
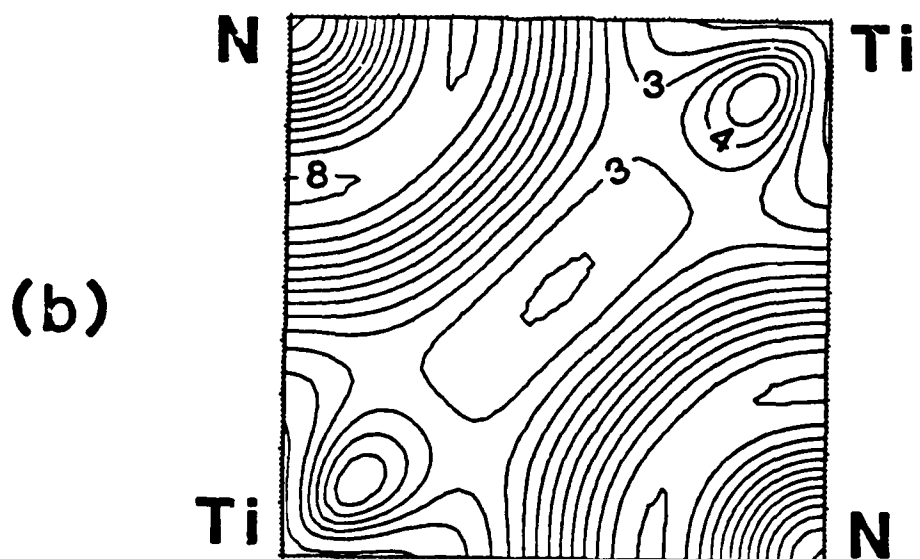
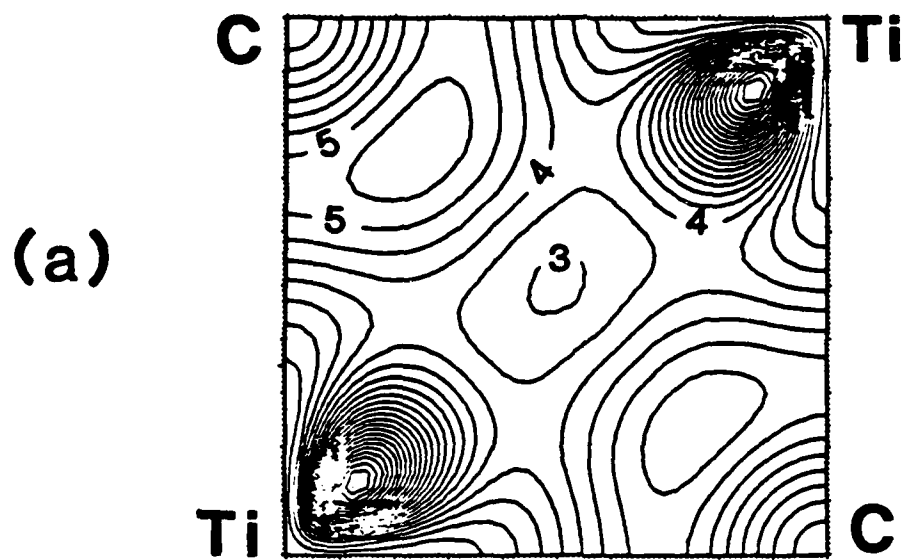


FIG. 7

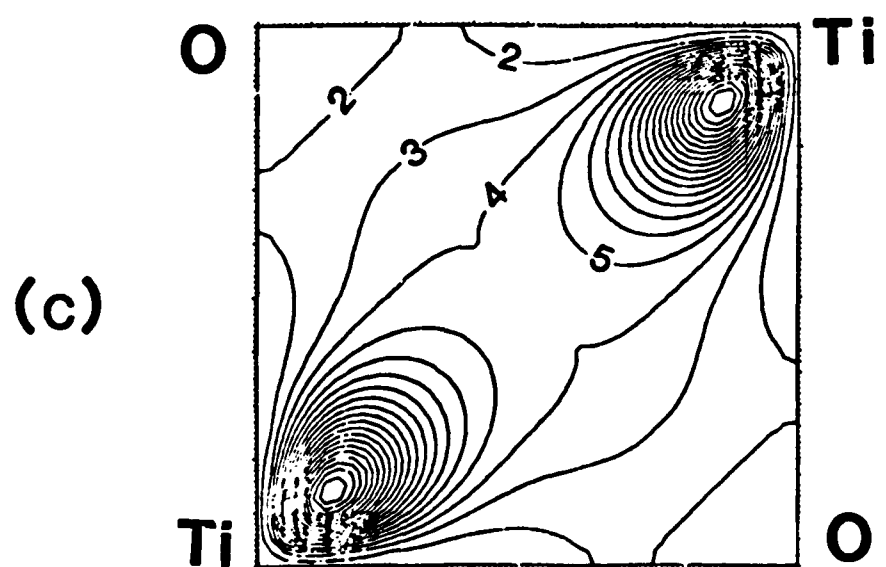
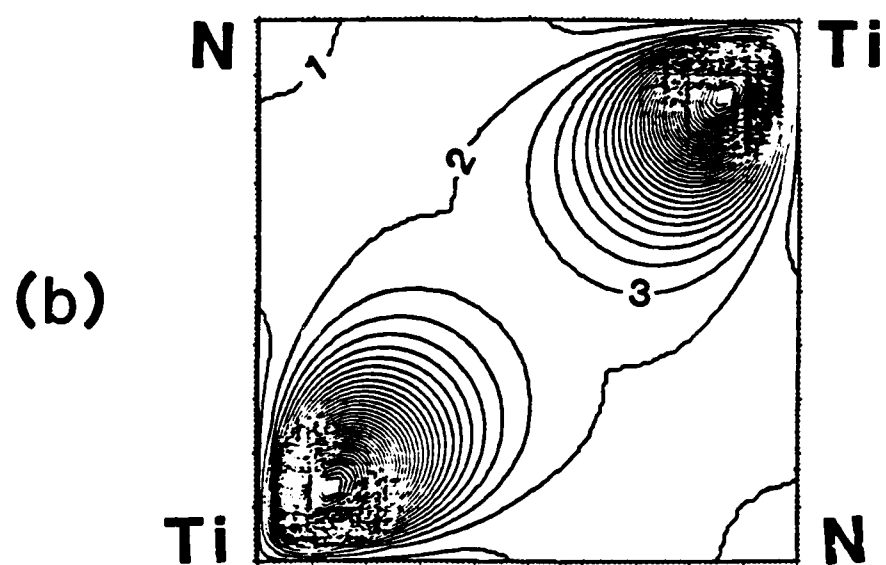
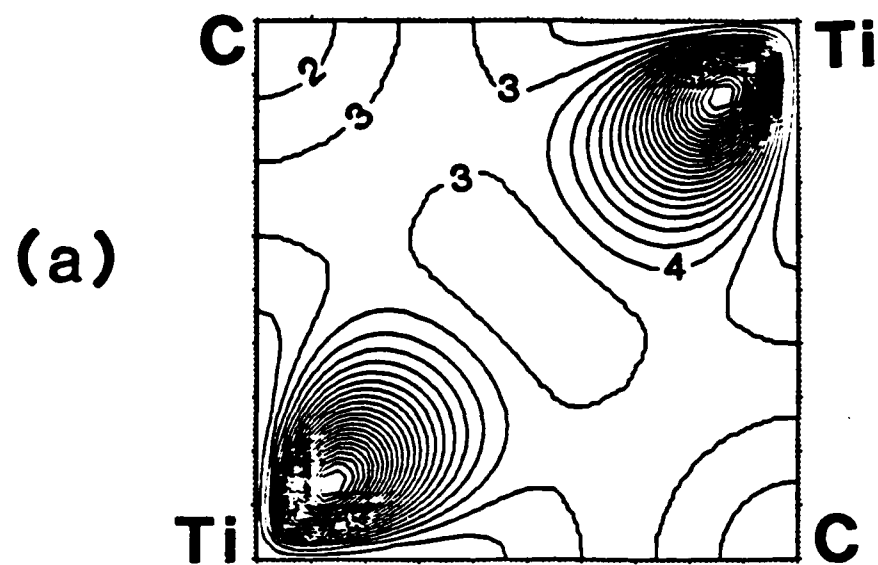


FIG. 8

END

12-86

DTIC